

**A NEW *IN SITU* METHOD OF DETERMINING RELATIVE ABUNDANCES AND CHARGE STATES OF IMPLANTED TRANSITION METALS IN INDIVIDUAL GRAINS USING SYNCHROTRON X-RAY FLUORESCENCE.** K. Kitts<sup>1</sup>, S. Sutton<sup>2,3</sup> and M. Newville<sup>3</sup>, <sup>1</sup>Department of Geology & Environ. Geosciences, Northern Illinois University (Davis Hall 312, Normal Rd, DeKalb, IL 60115; kkitts@niu.edu), <sup>2</sup>Department of Geophysical Sciences and <sup>3</sup>Center for Advanced Radiation Sources (University of Chicago, Chicago, IL 60637).

**Introduction:** In order to determine *in situ* the relative abundances and charge states of the transition metals in implanted solar wind in individual lunar plagioclase grains (see accompanying abstract [1]), we have developed a new microbeam x-ray fluorescence method using the synchrotron x-ray microprobe at the Advanced Photon Source (GSECARS sector 13) at Argonne National Laboratory.

**Materials and Beam Description:** Under clean laboratory conditions, solar wind implanted plagioclase grains from various lunar soils were hand-picked as described in [2], mounted on an acrylic rod and placed in the x-ray beam. The x-ray beam was derived from an APS undulator with the gap set to supply 10.35 keV photons at the undulator fundamental. A cryogenic Si (111) double-crystal monochromator was used to narrow the energy bandwidth of the beam. A combination of focusing mirrors in a Kirkpatrick-Baez geometry and slits produced a 3 x 3  $\mu\text{m}$  x-ray beam containing  $\sim 10^{12}$  photons/sec.

**Method Description:** XRF analyses were obtained in grazing incidence geometry where the angle between the incident x-ray beam and the crystal face was less than 1 degree. This geometry is used to maximize the fluorescence signals from the solar wind implanted material (peak implantation depth  $\sim 200$  nm) [3].

For atomically-flat surfaces, x-ray reflectivity can be used to set the incident angle with millidegree accuracy [4]. However, the typical roughness of lunar crystal surfaces presents a less than ideal situation in this regard (see figure 1).

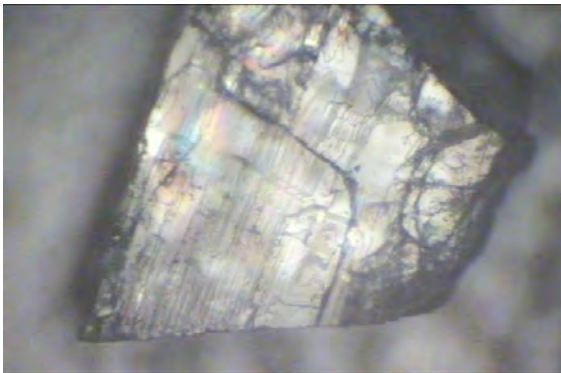


**Figure 1.** Optical photograph of a lunar plagioclase grain ( $\sim 200$  microns) mounted for XRF analysis showing typical surface roughness.

Our analytical approach was to align each crystal face as close to grazing incidence as feasible, typically at an incidence angle of  $\sim 0.5$  deg. At 0.5 deg, the absorption depth for 10.35 keV x-rays (incident beam energy) in anorthite is  $\sim 1$   $\mu\text{m}$ . The absorption depths for the fluorescence x-rays (near normal exit to the detector) are 13, 23, 31, 37, and 57  $\mu\text{m}$  for Ca, Cr, Mn, Fe, and Ni, respectively. Consequently, the analysis geometry is in the thin sample regime where all of the implanted solar ions for these elements are excited and absorption of their fluorescence x-rays is negligible. The element concentrations determined are averaged over  $\sim 1$   $\mu\text{m}$  thickness which means they are diluted from the concentrations in the implant region only. These dilution factors are difficult to determine accurately so we relied on relative concentrations.

Because, x-ray reflectivity was not suitable for these high roughness surfaces, the procedure used to set the crystal face in grazing incidence geometry was based on the transmission intensity profile for the incident beam as the crystal was scanned through the beam, i.e., a knife-edge scan. Such a profile will be a step function when the beam is parallel to the crystal surface.

At non-parallel orientations, the transmission profile is broadened by the partial absorption by the crystal at the onset of beam occultation. This angular dependence is best observed using the derivative of the profile which becomes an intense, narrow peak at optimal alignment. This effect can be demonstrated analytically. Consider a crystal face on an anorthite, right angle block at an angle  $\theta$  to the incident beam. The x-ray absorption by the crystal is characterized by the linear attenuation coefficient  $\mu$  ( $= 70$   $\text{cm}^{-1}$  at 10.35 keV). At a ray where the beam intersects the crystal, the transmission factor  $I$ , defined as the ratio between the downstream ion chamber signal and the upstream ion chamber signal normalized to the ratio for an air path, is given by,

$$I(x) = \exp(-\mu L(x))$$

where  $L(x)$  is the beam path length through the crystal at lateral position  $x$

$$L(x \geq 0) = x \sqrt{\frac{1}{\sin^2 \theta} + \frac{1}{\cos^2 \theta}}$$

( $x$  is defined to be zero at the crystal corner). The beam intensity cross section in this one-dimensional system is a Gaussian distribution  $G(x, \sigma)$ ,  $\sigma$  is its standard deviation =  $FWHM/2.35$ . Thus, the transmitted beam profile  $T(x)$  is

$$T(x) = \int_{-x}^{+x} I(x)G(x)dx$$

where the crystal is scanned through the beam from  $-X$  to  $+X$ . Figure 2 shows an example using  $\sigma = 3 \mu\text{m}$  and  $\mu = 70 \text{ cm}^{-1}$  over the angular range from  $0.5^\circ$  to  $5.0^\circ$  in  $0.5^\circ$  steps. This shows the decrease in intensity, broadening and shift of the profile with increasing angle. The x-ray transparency of the crystal causes an asymmetry on the crystal side of the profile.

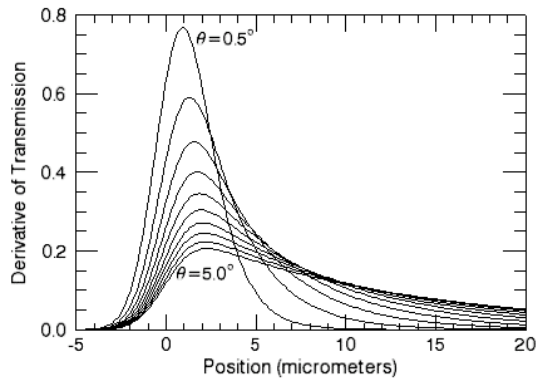


**Figure 2.** Theoretical beam transmission profiles (derivatives) showing the decrease in intensity, increase in peak width and shift of the profile with increasing angle.

Figure 3 shows data acquired from a crystal from Apollo 17 (70181) showing similar behavior. The positional shift between the profiles is due to the crystal surface being slightly displaced from the rotation axis. Based on these data, the XRF spectrum was collected at a rotational stage angle of zero degrees at a translation stage position of  $0 \mu\text{m}$  for this surface.

The approach used in this work was to obtain XRF analyses in the grazing incidence geometry described above (implantation plus bulk signal) and  $45 \text{ deg}$  geometry (bulk dominated) and subtract the two compositions (in element wt %) to obtain the surface-correlated elemental concentrations (solar wind implanted in lunar plagioclase in our application here). Concentrations were determined using the NRLXRF program [5] using calcium as an internal reference element (i.e., Ca concentration assumed based on An95 stoichiometry). The surface-correlated concentrations are then normalized to Fe to produce relative concentrations.

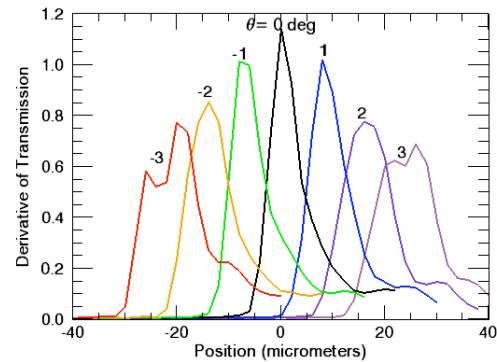


**Figure 3.** Apollo 17 plagioclase crystal alignment intensity derivative. The vertical axis is the derivative of the transmission signal and the horizontal axis is the position of the crystal translation stage. Profiles are shown for 6 positions (-3 to +3 degrees) of the crystal rotation stage.

Charge states for these implanted elements can also be determined using microXANES. MicroXANES spectra can be collected in the grazing incidence geometry sequentially with the XRF spectra by scanning the incident beam energy through the absorption edge of the element of interest and measuring the fluorescence intensity. These spectra are then compared to those measured for oxidation state standards.

Results of applying this method to solar wind implanted lunar plagioclase grains are described in an accompanying abstract [1].

**References:** [1] Kitts et al., (2007) this volume. [2] Kitts et al., (2003) *Geochim. et Cosmochim. Acta*, **67**, 4881-4893. [3] Jull and Pillinger, (1977) *Proc. Lunar Sci. Conf.* **8**, 3817-3833. [4] Eng et al. (2001) *Science*, **288**, 1029-1033. [5] Criss, (1979), *Applied Spectroscopy*, **33**, pp.19-25.

**Acknowledgements:** GeoSoilEnviroCARS is supported by NSF-Earth Sciences (EAR-0622171) and DOE-Geosciences (DE-FG02-94ER14466). Use of the Advanced Photon Source was supported by the U. S. Department of Energy, Office of Science, Office of Basic Energy Sciences, under Contract No. DE-AC02-06CH11357.